Preferential electrosorption of cobalt (II) tetra-aminophthalocyanine at single-wall carbon nanotubes immobilized on a basal plane pyrolytic graphite electrode

Kenneth I. Ozoemena, Jeseelan Pillay and Tebello Nyokong

Abstract

This communication describes the preferential electrosorption of cobalt (II) tetra-aminophthalocyanine (CoTAPc) (rather than the expected electropolymerisation) onto a SWCNT immobilized on a basal plane pyrolytic graphite electrode (BPPGE). Cyclic voltammetric and electrochemical impedance spectroscopic data revealed that the electrosorbed CoTAPc is highly stable, well organized with comparable electron-transfer rate constant in ferricyanide solution ($k_{app} \sim 6 \times 10^{-5}$ cm s^{-1} order) to that of the SWNCT. Electrochemical kinetics of the electrosorbed CoTAPc yielded k_s of 0.169 s^{-1} and 832.2 s^{-1} for the cathodic and anodic reactions, respectively, indicative of different rate-determining steps for the cathodic and anodic reactions. Strong π-stacking interactions between CoTAPc and the sidewalls of the SWCNTs, with possible synergistic covalent interactions, are explained as responsible for the preferential electrosorption process. Both BPPGE-SWCNT-CoTAPc$_{(ads)}$ and BPPGE-SWCNT showed comparable electrocatalytic responses towards the detection of 2-(diethylamino) ethanethiol (DEAET).

1. Introduction

Carbon nanotubes (CNTs), single-walled (SWCNTs) or multi-walled (MWCNTs), exhibit unusual electrical conductivity, adsorption properties, and chemical stability and are ideal for constructing efficient electrochemical sensors [1] and [2]. A recent study by Banks et al. [3] proved that the "electrocatalytic" properties of CNTs are due their inherent metallic impurities that cannot be removed even by acid-washing. In addition, CNTs possess highly π-conjunctive and hydrophobic sidewalls consisting of sp^2 carbons and open ends bearing oxygen-containing moieties that actually allow them to function as support for organic and inorganic electrocatalysts. Transition metal phthalocyanine (MPc) complexes (e.g., CoPc and its derivatives), versatile class of organic macrocycles with 18 π-electrons, have continued to establish themselves as excellent electrocatalysts suitable for the fabrication of electrochemical sensors [4] and [5]. Facile coordination of these two remarkable π-electron species may revolutionize their applications as electrocatalysts and in the fabrication of high-performance electrochemical sensors. Carbon electrode modifications with tetra-aminometallophthalocyanine (MTAPc) and related metalloporphyrin (MTAP) complexes are performed via electropolymerisation process because of the ease with which these amino-derivatized complexes undergo electropolymerisation at such electrodes. Electrodes modified with CoTAPc, in particular, have received much attention because of the high electrocatalytic activities of this macromolecule. Electropolymerisation has long been recognized as the facile method for the modification of carbon electrodes with MTAPc complexes due to the ease at which they electropolymerize at carbon electrodes [4], [5], [6], [7] and [8]. Electrochemical techniques provide better insights into the adsorption and reactivity of surface-confined redox-active species than other known analytical techniques. This work reports the preferential electrosorption rather than electropolymerisation of CoTAPc at SWCNT-modified BPPPGE. Electrosorption (i.e., chemical adsorption or chemisorption of a species from solution on the surface of an electrode whose potential is controlled [9]) is important in electrode fabrication since the amount of adsorbed species can be controlled. Adsorption of MPc [10] and [11] and its related metalloporphyrin [12] and [13] complexes onto the walls of CNT via π–π interactions have been observed spectroscopically. To the best of our knowledge, this is the first time electrosorption of any MPc complex with CNTs has been observed, thereby demonstrating that this is a useful and potentially versatile means of coordinating SWCNTs with a wide range of substituted MPc and related organic macrocycles for fundamental and practical electrochemical studies. We used electrochemical impedance spectroscopy (EIS) to probe the physico-chemical properties of these surface–confined complexes. Preliminary electrocatalysis is also described.

2. Experimental

2.1. Materials and reagents

Single-walled carbon nanotubes (SWCNTs) were obtained from Aldrich, and converted to short and uncapped nanotubes bearing acidic functions (SWCNT-COOH) following the established multi-step acid treatment procedures [14], simply referred to in this work as SWCNT. Cobalt tetra-aminophthalocyanine (CoTAPc) complex was synthesized and characterized according to established procedures [15]. Cobalt phthalocyanine (CoPc) was obtained from Aldrich and used as supplied. 2-(Diethylamino)ethanethiol (DEAET) was obtained from Sigma. Ultra pure water of resistivity 18.2 MΩ was obtained from a Milli-Q Water System (Millipore Corp., Bedford, MA, USA) and was used throughout for the preparation of solutions. Phosphate buffer solutions (PBS) at various pHs were prepared with appropriate amounts of K_2HPO_4 and KH_2PO_4, and the pH adjusted with 0.1 M H_3PO_4 or NaOH. All electrochemical experiments were performed with nitrogen-saturated PBS. All other reagents were of analytical grades and were used as received from the suppliers without further purification.

2.2. Apparatus and procedure

Electrochemical experiments were carried out using an Autolab Potentiostat PGSTAT 30 (Eco Chemie, Utrecht, The Netherlands) driven by the GPES software version 4.9. Electrochemical impedance spectroscopy (EIS) measurements were performed with an Autolab FRA software between 1.0 Hz and 10 kHz using a 5 mV rms sinusoidal modulation with a solution of 1 mM of $K_4Fe(CN)_6$ and 1 mM $K_3Fe(CN)_6$ (1:1) mixture containing 0.1 M KCl, and at the $E_{1/2}$ of the $[Fe(CN)_6]^{3-/4-}$ (0.124 V vs. Ag|AgCl). Bare or modified basal plane pyrolytic graphite (BPPGE) disk (d = 5 mm in Teflon) was used as the working electrode and was fabricated in-house from BPPG plate (Le Carbone, Sussex, UK). Electrical contact with the disk was maintained through an inserted copper wire held in place with conducting silver varnish L 100 (Kemo® Electronic, Germany). A Ag|AgCl wire and platinum wire were used as pseudo-reference and counter electrodes, respectively. A WTW pH 330/set-1 (Germany) pH meter was used for pH measurements. All solutions were de-aerated by bubbling nitrogen prior to each electrochemical experiment. Experiments were performed at 25 ± 1 °C.

2.3. Electrode modification and pretreatments

The BPPGE surface was first cleaned as reported before [16] by gentle polishing on a p1200C Norton carborundum paper (Saint-Gobain Abrasives, Isando, South Africa), followed by cleaning with cellotape process of removing graphite layers and finally rinsing in acetone to remove any adhesive. The CoTAPc- or CoPc-modified BPPGE-SWCNT was obtained by immersing a BPPGE-SWCNT (obtained by drop-dry method) in a solution of 10^{-3} M CoTAPc (or CoPc) in dry DMF containing 10^{-2} M tetrabutylammonium tetrafluroroborate (TBABF$_4$) as the supporting electrolyte and repetitively scanned (50 scans) using cyclic voltammetry. For simplicity, the CoTAPc- or CoPc-modified BPPGE-SWCNT are herein abbreviated as BPPGE-SWCNT-CoTAPc$_{(ads)}$ and BPPGE-SWCNT-CoPc$_{(ads)}$, respectively. The modified electrodes were pretreated by immersing in a 0.1 M PBS of either pH 4.0 or pH 7.0, and the solution scanned between −1.0 V and 1.0 V or −1.0 V and 0.3 V (vs. Ag/AgCl) for 20 cycles to obtain a stable cyclic voltammogram.

3. Results and discussion

3.1. Electrosorption behaviour and aqueous pre-treatment

Fig. 1 presents typical voltammetric responses obtained during the continuous scanning of the DMF solutions of CoTAPc (and CoPc (inset)) containing TBABF$_4$. For the CoTAPc, both cathodic and anodic voltammetric waves decreased continuously from the first scan and then remained stable until about the 30th scan when peaks (I) and (III) finally disappeared. This behaviour exhibited by CoTAPc is characteristic of electrosorption process [17] and [18] and clearly suggest the continuous interaction or attachment of the CoTAPc onto the BPPGE-SWCNT forming the BPPGE-SWCNT-CoTAPc$_{(ads)}$. The final CV obtained after the completion of the electrosorption process was highly reproducible and electrochemically stable. This observation is interesting in that MTAPc

complexes easily undergo electropolymerisation onto surfaces of carbon electrodes [4], [5], [6], [7], [8] and [9] and BPPGE-MWCNT [19]. The preferential electrosorption of CoTAPc may be related to the special features of the SWCNTs over MWCNTs such as smaller size, larger specific area (more than a magnitude [20]), stronger inter-tube attraction and adsorptive properties. In fact, SWCNTs have characteristic curve-shaped surface that facilitates bonding of supramolecular complexes via non-covalent or hydrophobic interactions [12]. Thus, the reproducibility of the electrosorption trend may be the result of highly efficient or intense adsorption of the CoTAPc onto the SWCNT by π–π interaction between the benzene rings of the phthalocyanine and the sidewalls of the immobilized SWCNT particle. CoPc (i.e., without amino substituent as the CoTAPc) was employed in this study to provide some insights as to the possible influence of the –NH$_2$ functionality on the observed electrosorption process. Thus, the ill-resolved and weak eletrosorption process for the CoPc (Fig. 1 inset) suggests that with CoTAPc there might be some additional types of interaction involving the –NH$_2$ functionality of the CoTAPc. We have no meaningful explanation at this moment as to how such electrochemical process occurs, but could very likely involve electrochemical-induced radical formation, radical–radical coupling, and/or bonding. From literature precedences [4], [5], [6], [7], [8] and [9], peaks (II) and (IV) are attributable to Co(II)/Co(I) and Co(III)/Co(II) processes, respectively. Peaks (I) and (III) are due to the Pc ring processes. The total collapse of the peaks (I) and (III) during electrosorption is indicative of the involvement of the Pc rings rather than the cobalt centre.
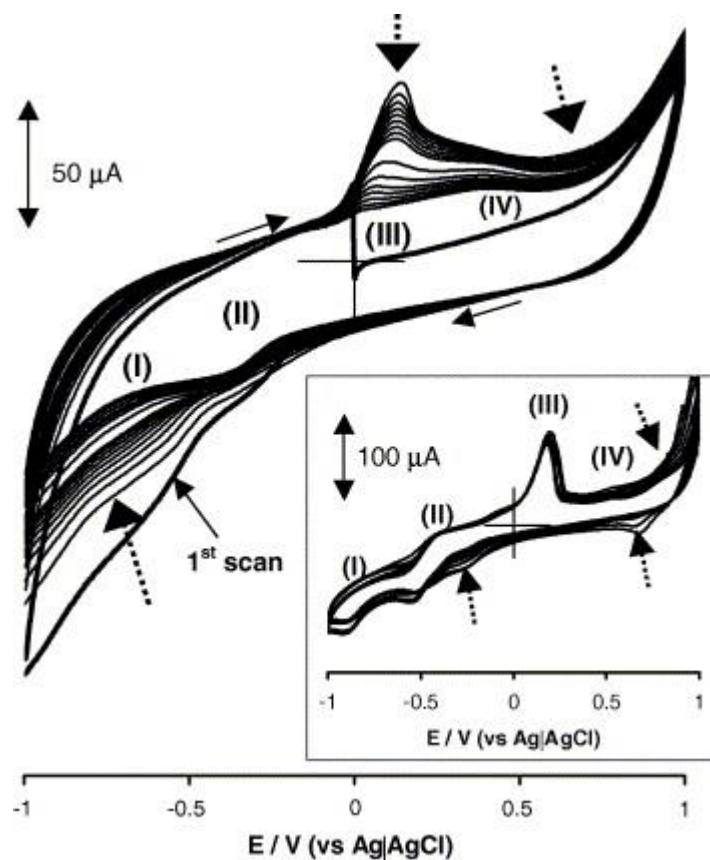

Fig. 1. Repetitive cyclic voltammetric profiles at 50 scans (1st and every 5th scan recorded, outer to inner) of a 1 mM CoTAPc in DMF containing TBABF$_4$ at a BPPGE-SWCNT. Inset shows similar experiment with CoPc. Scan rate = 50 mV/s. Broken arrows indicate the direction of voltammetric responses.

During pretreatment of the electrosorbed film in aqueous solution (Fig. 2), interestingly, we observed well defined continuous growth of a reversible redox couple (with peaks at +0.22 V and −0.12 V vs. Ag|AgCl) for the BPPGE-SWCNT-CoTAPc$_{(ads)}$, exhibiting peak current ratio (I_{pa}/I_{pc}) of one, with a peak separation (ΔE_p) of ca.0.34 V (vs. Ag|AgCl) and half-wave potential ($E_{1/2}$) of 0.05 V (vs. Ag|AgCl). The two waves were dependent of each other as none occurred without the other. Similar CV evolutions also occurred at wide potential window with the Co(III)/Co(II) peak found at 0.4 V (not shown). This rarely observed behaviour could be ascribed to the re-arrangement of electrosorbed CoTAPc film on the BPPGE-SWCNT surface. After the 20th scan, the CV remained stable and started to decrease, signifying the end of the rearrangement. Fig. 2 inset (a) reveal a stable Co(II)/Co(I) redox couple (I). Fig. 2 inset (b) compares the CVs obtained in PBS pH 4.4 for the bare (i), BPPGE-

SWCNT (ii) and the conditioned electrode (iii). As evident in Fig. 2 (inset (a), curve ii), the intrinsic redox processes of the SWCNT [21] and [22] are not properly resolved at the BPPGE, it is reasonable to imply that the obtained voltammogram for the SWCNT-CoTAPc (iii), especially the broad cathodic peak, may be due to the overlap of the redox processes of the SWCNT, the phthalocyanine ring as well as the irreversible Co(I)/Co(II). The plot of $E_{1/2}$ against pH (investigated with SWV at pH 2–10) resulted in a slightly higher slope ($\sim$ −70 mV/pH) than the theoretical value of $\sim$60 mV/pH, which might have been influenced by the overlapped redox processes mentioned above. The surface coverage was estimated as $\sim$1.0 × 10^{-9} mol/cm^2, a magnitude higher than a monolayer coverage, indicating that the obtained film is about a magnitude denser than a monolayer film.
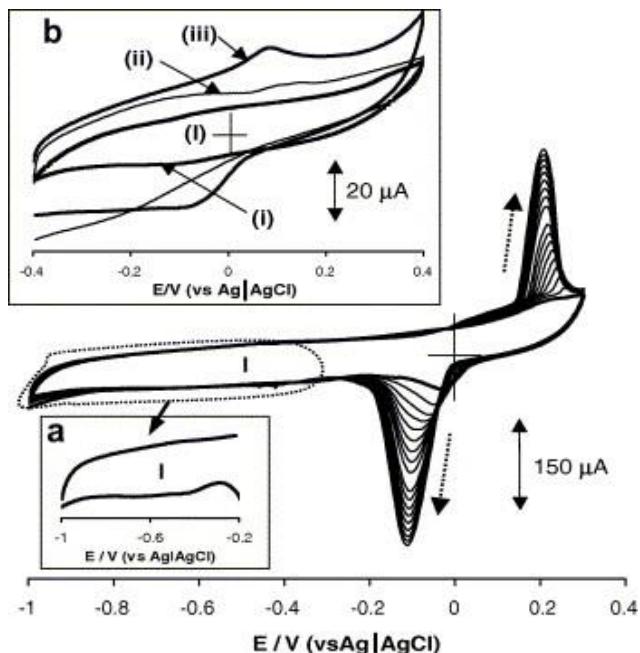

Fig. 2. Repetitive cyclic voltammetric profiles of a BPPGE-SWCNT-CoTAPc$_{(ads)}$ in PBS (pH 7.0), 1st to 20th scans (inner to outer voltammograms). Inset (a) shows the Co(II)/Co(I) couple. Inset (b) is the comparative CVs of: (i) bare BPPGE, (ii) BPPGE-SWCNT and (iii) BPPGE-SWCNT-CoTAPc$_{(ads)}$ in PBS (pH 4.4). Scan rate = 50 mV/s.

3.2. Electrochemical kinetics of the electrosorbed CoTAPc film

Fig. 3 shows typical CV evolution at varying rates (25–1500 mV/s) of the pre-treated BPPPGE-SWCNT-CoTAPc$_{(ads)}$. The redox currents resulted in a linear increase with scan rates at low scan rates, expected for surface-immobilized redox species. At scan rates >100 mV/s, the cathodic peak became severely distorted, shifting to more negative potentials compared to the positive shifts recorded for the anodic wave at similar scan rates, suggesting irreversibility at high scan rates. Following the Laviron's theory for irreversible electrode reactions [23], plots of E_p vs. ln v (inset) yielded $\alpha n = 0.125$ with $k_s = 0.169$ s^{-1} for the cathodic reaction, and $(1 - \alpha)n = 0.33$ with $k_s = 832.2$ s^{-1} for the anodic reaction. These data suggest that the rate-determining steps of the cathodic and anodic reactions might be different. The small k_s value for the cathodic reaction is indicative of weak electron transfer process arising from the complications of the overlapped reactions. This behaviour where one redox wave exhibits higher peak current than its reverse wave is typical for CoPc and its complexes [24].
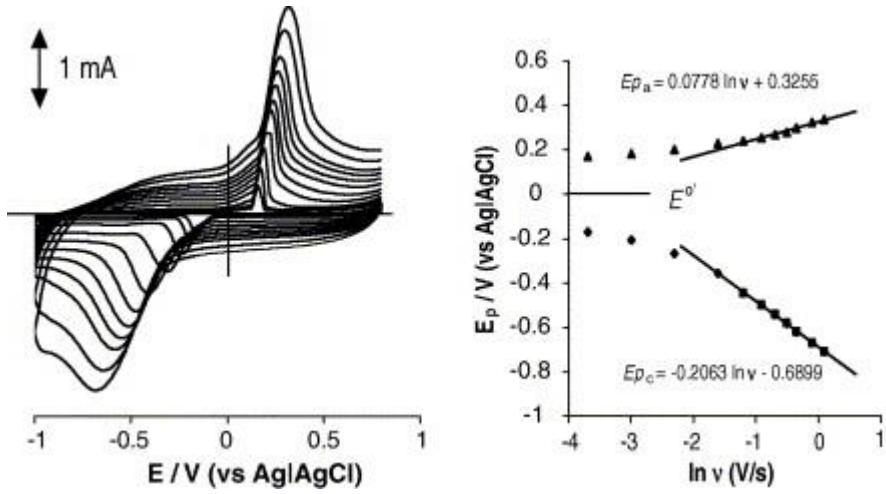
Fig. 3. Effect of varying scan rates (25–1500 mV/s inner to outer) of a BPPGE-SWCNT-CoTAPc$_{(ads)}$ in PBS (pH 4.4). Inset is the plot of E_p vs. ln v.

3.3. Electrochemical impedance spectroscopy (EIS)

Electrochemical impedance spectroscopy (EIS) is an effective technique for probing the redox and structural features of a surface-confined species [25]. Prior to EIS experiments, comparative CVs of the $[Fe(CN)_6]^{3-/4-}$ redox probe were obtained (Fig. 4a). Unlike the bare BPPGE (i), modified BPPGEs (ii–v) gave well-defined redox peaks with approximately same current responses. The Co$^{(II)/(III)}$ redox couple for the CoTAPc was evident at 0.37 V (vs. Ag|AgCl) (see wave iv of inset, Fig. 4a) further confirming the successful attachment of this redox-active MPc complex film onto SWCNT. The Nyquist plots ($Z_{imaginary}$ vs. Z_{real}) exhibited the characteristics semicircles (most pronounced for the bare (i) than the modified BPPGEs (ii–v)) at high frequencies and a straight line at low frequencies, corresponding to kinetic and diffusion processes, respectively. The estimated EIS parameters from the constant phase element (CPE) equivalent circuit model (i.e., $R_s - R_{et}$//CPE, where R_s is the solution resistance, R_{et} is the electron-transfer resistance [24] and [26]) are listed in Table 1. The modified BBPGEs showed parallel lines at low frequencies suggesting similarities in the diffusional behaviour of $[Fe(CN)_6]^{3-/4-}$ at these electrodes. A significant decrease in the R$_{et}$ value for the modified electrodes compared to the bare BPPGE confirm that the charge transfer processes on the modified electrodes for $[Fe(CN)_6]^{3-/4-}$ are easier than in the bare BPPGE. The weak CV response for BPPGE towards $[Fe(CN)_6]^{3-/4-}$ are consistent with reports [2] and could be associated with its roughness and/or basal nature, thus the consequent high R$_{et}$ is not surprising. The R$_{et}$ values for the BPPGE-SWCNT and BPPGE-SWCNT-CoTAPc$_{(ads)}$ are consistent with step-wise build-up of the layers on the BPPGEs. The high CPE value for BPPGE-SWCNT-CoTAPc$_{(ads)}$ reflects the more uniform or homogenous nature of the electrode compared to others [26]. The similarity of the rate constants for BPPGE-SWCNT and BPPGE-SWCNT-CoTAPc$_{(ads)}$ demonstrates the efficiency of the SWCNT to function as molecular wires, i.e., the SWCNTs do not add significant electrical resistance. These results corroborate the CVs of Fig. 4. The structural differences are further confirmed from the Bode plots (θ (phase angle) vs. log f (frequency)). Bare BPPGE showed symmetrical peak with a maximum value of $\sim 41°$ at 372 Hz corresponding to the relaxation process of the BPPGE|solution interface. Modification of the BPPPGE led to the disappearance of this relaxation with new ones observed at different maxima. The BPPGE-SWCNT-CoTAPc$_{(ads)}$ exhibited much larger maximum of relaxation (46° at 7 Hz) with better defined and narrower distribution peak compared to those of the other modified electrodes, a clear indication that the electrosorbed CoTAPc film on the SWCNT surface is denser with more regular structures than others. These data corroborate the CPE values discussed above.
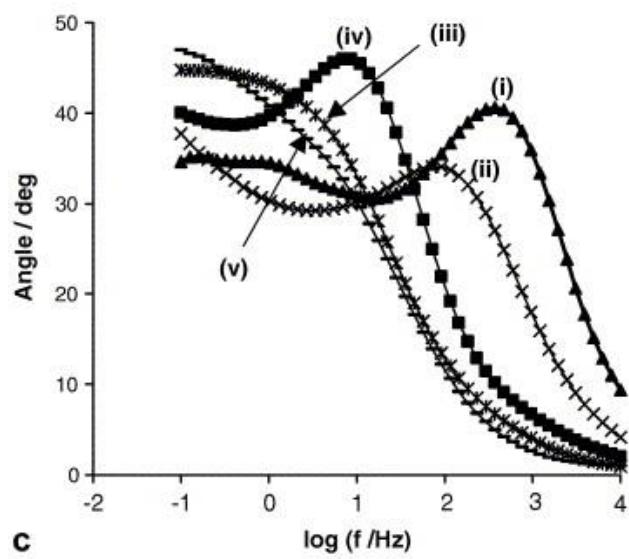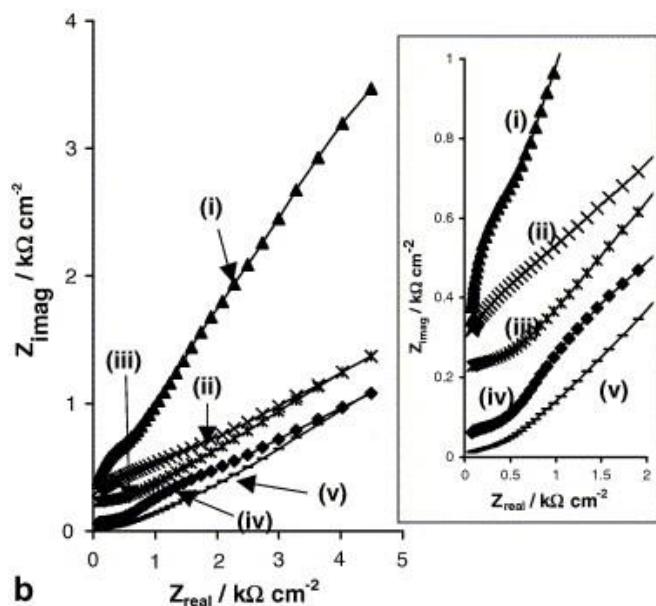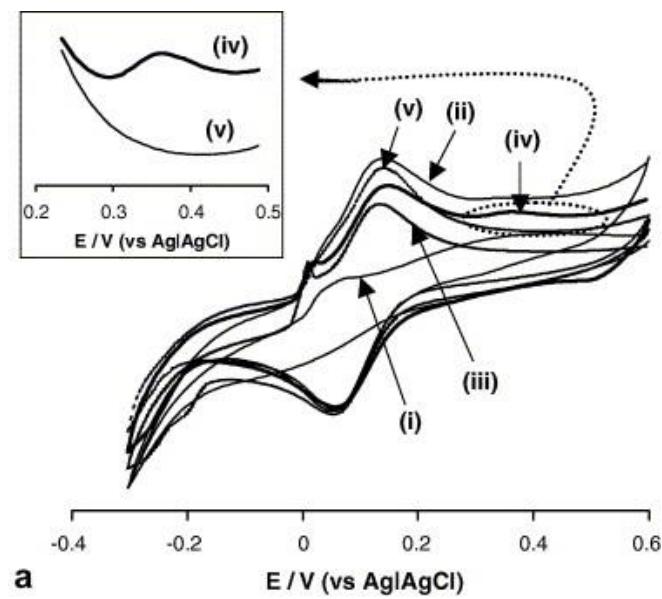
Fig. 4. CV profiles of $[Fe(CN)_6]^{3-/4-}$ at 25 mV/s (a), Normalized Nyquist (b) and Bode (c) plots resulting from bare BPPGE (i), BPPGE-CoTAPc (ii), BPPGE-SWCNT-CoPc$_{(ads)}$ (iii), BPPGE-SWCNT-CoTAPc$_{(ads)}$ (iv) and BPPGE-SWCNT (v) in 0.1 M KCl containing equimolar mixture of $K_4Fe(CN)_6$ and $K_3Fe(CN)_6$. Inset (a) shows Co(III)/Co(II) couple. Inset (b) shows Nyquist plots at the high frequency region.

Table 1.

Summary of estimated EIS data obtained for the electrodes

Electrodes	$R_s/\Omega\ cm^{-2}$	$R_{et}/k\Omega\ cm^{-2}$	$CPE/\mu F\ cm^{-2}$	$k_{app}/cm\ s^{-1}$
Bare BPPGE	273.50	8.05	0.255	3.31×10^{-5}
BPPGE-CoTAPc	269.42	2.60	5.81	10.24×10^{-5}
BPPGE-SWCNT	459.38	3.88	77.41	6.85×10^{-5}
BPPGE-SWCNT-CoPc$_{(ads)}$	420.07	0.36	5.33	73.93×10^{-5}
BPPGE-SWCNT-CoTAPc$_{(ads)}$	276.04	4.23	116.12	6.30×10^{-5}

3.4. Possible application to electrocatalytic detection

For some insights into the electrocatalytic potential of the electrodes, DEAET, a thiol hydrolysis product of V-type nerve agent [27] was chosen as an important analytical probe. BPPGE-SWCNT and BPPGE-SWCNT-CoTAPc$_{(ads)}$ exhibited catalytic response (enhanced current at less positive potential) while the other electrodes exhibited little or no detectable catalytic response for this analyte. As observed recently for MWCNT [3], we can ascribe the "electrocatalysis" seen at the BPPGE-SWCNT mainly to the inherent metallic impurities of SWCNT. The poor activity of the BPPGE-SWCNT-CoPc$_{(ads)}$ over BPPGE-SWCNT-CoTAPc$_{(ads)}$ is somewhat surprising but may be rationalized as follows. SWCNT is a well-known electron-acceptor [12] and [13] and CoTAPc is more electron-donating (by virtue of the lone pair electrons on the $-NH_2$ substituent) than unsubstituted CoPc. Thus, CoTAPc acts as a more viable reaction center than CoPc while SWCNT facilitates the necessary electron transport. The CV of DEAET with BPPGE-SWCNT showed two peaks, one at about 0.50 V, and the other at about 0.74 V. Such double oxidation peaks have been observed before for CNT-based electrodes during electrocatalytic detection of thiol-containing analytes [28]. Based on such reports, we ascribe the first oxidation peak (at ~0.48 V) to be mediated by the quinone-like functional groups at the tube ends of the SWCNT, while the second oxidation peak (at ~0.74 V) to be mediated by the edge plane-like carbon at the SWCNT [27]. On BPPGE-SWCNT-CoTAPc$_{(ads)}$ (Fig. 5(iv)), one sharp peak corresponding to DEAET oxidation was observed at less potential (+0.58 V) with enhanced current compared to the BPPGE-CoTAPc, indicating that SWCNT-CoTAPc$_{(ads)}$ greatly improves the electronic communication between the DEAET and the BPPGE. Plot of anodic peak current (I_{pa}) against the square root of scan rate ($v^{1/2}$) (for scan rates less than 300 mV/s, figure not shown) resulted in a straight line, an indication of a diffusion controlled DEAT oxidation.
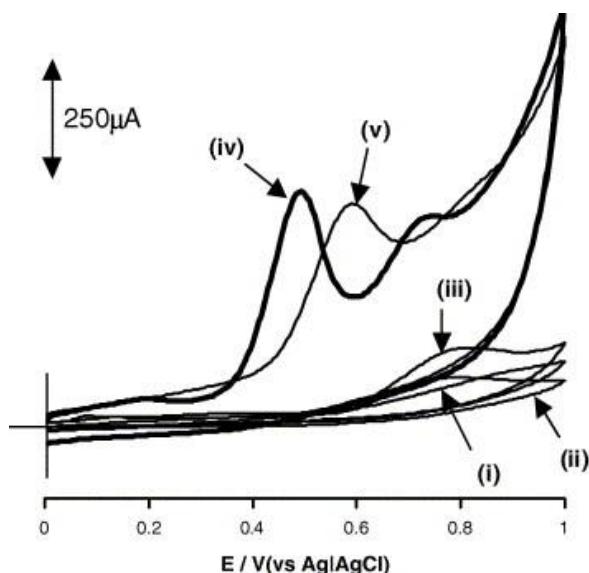

Fig. 5. Typical comparative cyclic voltammograms for 1.2 mM DEAET in pH 7.0 PBS at different electrodes; (i) bare BPPPGE, (ii) BPPGE-SWCNT-CoPc$_{(ads)}$, (iii) BPPGE-CoTAPc (iv) BPPGE-SWCNT-CoTAPc$_{(ads)}$ and (v) BPPGE-SWCNT. Except for (ii and iv), all other electrodes were obtained by drop-dry method. Scan rate = 50 mV/s.

4. Conclusion

We have described the electrochemical interaction between CoTAPc and surface-confined SWCNTs. The strong π-stacking interaction between the adsorbed CoTAPc and the sidewalls of the SWCNTs is regarded as responsible for the preferential electrosorption process. EIS experiments proved that this electrosorptive interaction leads to a denser and more organized redox-active film structure, with good potential for electrocatalytic detection of hydrolysis product of V-type nerve agent. This type of electrode modification with SWCNT may apply to other MTAPc and MTAP complexes, and can provide opportunity for controlled fabrication of sensors. The use of complementary techniques (such as optical and microscopic methods) to gain further insights to some of the questions raised in this work are being explored in our laboratories, and will be reported elsewhere.

Acknowledgement

References

[1] M. Musameh, J. Wang, A. Merkoki and Y. Lin, *Electrochem. Commun.* 4 (2002), p. 743.

[2] C.E. Banks, R.R. Moore, T.J. Davies and R.G. Compton, *Chem. Commun.* (2004), p. 1804.

[3] C.E. Banks, A. Crossley, C. Salter, S.J. Wilkins and R.G. Compton, *Angew. Chem. Int. Ed.* 45 (2006), p. 2533.

[4] J.H. Zagal, *Coord. Chem. Rev.* 119 (1992), p. 89

[5] K.I. Ozoemena and T. Nyokong In: C.A. Grimes, E.C. Dickey and M.V. Pishko, Editors, *Encyclopedia of Sensors* vol. 3, American Scientific Publishers, California (2006), pp. 157–200 (Chapter E).

[6] C.A. Caro, F. Bedioui and J.H. Zagal, *Electrochim. Acta* 47 (2002), p. 148.

[7] Y.-H. Tse, P. Janda, H. Lam, J.J. Zhang, W.J. Pietro and A.B.P. Lever, *J. Porphyr. Phthalocya.* 1 (1997), p. 3.

[8] H. Li and T.F. Guarr, *J. Chem. Soc., Chem. Commun.* (1989), p. 832.

[9] A.R. Ozkaya, I. Yilma and O. Bekaroglu, *J. Porphyr. Phthalocya.* 2 (1998), p. 483

[10] X. Wang, Y. Liu, W. Qiu and D. Zhu, *J. Mater. Chem.* 12 (2002), p. 1636.

[11] J.-S. Ye, Y. Wen, W.D. Zhang, H.F. Cui, G.Q. Xu and F.-S. Sheu, *Electroanalysis* 17 (2005), p. 89.

[12] T. Hasobe, S. Fukuzumi and P.V. Kamat, *J. Am. Chem. Soc.* 127 (2005), p. 11884.

[13] D.M. Guldi, G.M.A. Rahman, N. Jux, D. Balbinot, U. Hartnagel, N. Tagmatarchis and M. Prato, *J. Am. Chem. Soc.* 127 (2005), p. 9830.

[14] J. Liu, G. Rinzler, H. Dai, J.H. Hafner, R.K. Bradley, P.J. Boul, A. Lu, T. Iverson, K. Shelimov, C.B. Huffman, F. Rodrigues-Macias, Y.-S. Shon, T.R. Lee, D.T. Colbert and R.E. Smalley, *Science* 280 (1998), p. 1253.

[15] B.N. Achar, G.M. Fohlen, J.A. Parker and J. Keshavaya, *Polyhedron* 6 (1987), p. 1463.

[16] R.R. Moore, C.E. Banks and R.G. Compton, *Anal. Chem.* 76 (2004), p. 2677.

[17] X.-Y. Xiao and S.-G. Sun, *Electrochim. Acta* 45 (2000), p. 2897

[18] W. Yang, J.J. Gooding and D.B. Hibbert, *J. Electroanal. Chem.* 516 (2001), p. 10

[19] M.P. Siswana, K.I. Ozoemena, T. Nyokong, Electrochim. Acta in press.

[20] Y.-H. Yun, V. Shanov, M.J. Schulz, S. Narasimhadevara, S. Subramaniam, D. Hurd and F.J. Boerio, *Smart Mater. Struct.* 14 (2005), p. 1526

[21] H. Luo, Z. Shi, N. Li, Z. Gu and Q. Zhuang, *Anal. Chem.* 73 (2001), p. 915.

[22] C. Hu, X. Chen and S. Hu, *J. Electroanal. Chem.* 586 (2006), p. 77.

[23] E. Laviron, *J. Electroanal. Chem.* 101 (1979), p. 19.

[24] K.I. Ozoemena and T. Nyokong, *Electrochim. Acta* 51 (2006), p. 2669.

[25] E. Katz and I. Wilner In: V.M. Mirsky, Editor, *Ultrathin Electrochemical Chemo- and Biosensors. Technology and Performance*, Springer-Verlag, New York (2004), pp. 68–116 Chapter 4.

[26] J. Bisquert, G. Garcia-Belmonte, P. Bueno, E. Longo and L.O.S. Bulhoes, *J. Electroanal. Chem.* 452 (1998), p. 229.

[27] Y. Yang, *Acc. Chem. Res.* 32 (1999), p. 109.

[28] K. Gong, X. Zhu, R. Zhao, S. Xiong, L. Mao and C. Cheng, *Anal. Chem.* 77 (2005), p. 8158.